Journal of Integrative Agriculture 2026, 25(7): 3031–3043

Available online at ScienceDirect

Journal of Integrative Agriculture



RESEARCH ARTICLE

Warming alters fresh-carbon assimilating bacterial community relevant to priming effect in Mollisols

Yan Gao[1], Yansheng Li[1], Zhenhua Yu[1], Zhuxiu Liu[1], Jinyuan Zhang[1], Xiaojing Hu[1], Jun Wang[2], Hanting Cheng[3], Rong Li[4], Caixian Tang[5], Junjie Liu[1], Junjiang Wu[6], Guanghua Wang[1], Xiaobing Liu[1], Yueyu Sui[1], Jian Jin[1, 5#]

[1] *State Key Laboratory of Black Soils Conservation and Utilization, Northeast Institute of Geography and Agroecology, Chinese Academy of Sciences, Harbin 150081, China*

[2] *State Key Laboratory of Soil Erosion and Dryland Farming on the Loess Plateau, Institute of Soil and Water Conservation, Chinese Academy of Sciences and Ministry of Water Resources, Yangling 712100, China*

[3] *Environmental and Plant Protection Institute, Chinese Academy of Tropical Agricultural Sciences, Haikou 571101, China*

[4] *The Key Lab of Pollution Control and Ecosystem Restoration in Industry Clusters, Ministry of Education/South China University of Technology, Guangzhou 510006, China*

[5] *La Trobe Institute for Sustainable Agriculture and Food, Department of Ecological, Plant and Animal Sciences, La Trobe University, Bundoora, Vic 3086, Australia*

[6] *Key Laboratory of Soybean Cultivation of Ministry of Agriculture and Rural Affairs, Soybean Research Institute, Heilongjiang Academy of Agricultural Sciences, Harbin 150086, China*

Highlights

- Warming reversed the priming effect over time in Mollisol.
- Glucose-assimilating r-strategists changed to K-strategists under warming.
- Warming enriched Chloroflexi, contributing to positive priming effects.

Abstract

Soil microbial response to warming may potentially contribute to the positive priming effect, i.e., accelerating the decomposition of native soil organic carbon (SOC) under the outsourced carbon (C) input. Investigating microbiota that metabolize the outsourced C is essential to deciphering the mechanism of priming effect in response to warming and thus mitigating the SOC loss under warming climate. In this work, we monitored the priming effect at 25°C, 35°C and 45°C over four weeks with weekly addition of ^{13}C-glucose, and subsequently revealed microbial assemblage metabolizing glucose with the DNA stable-isotope probing (DNA-SIP) method. Warming initially inhibited the priming effect, and decreased bacterial α-diversity, K/r-strategists ratio (K/r) and recalcitrant C/labile C gene ratio (R/L) in week 1, suggesting that at the onset of the outsourced C input, the increased proportion of r-strategists preferentially utilize the added glucose over SOC to meet their C and energy demands. Yet, in week 4, positive priming effects were intensified by warming with up to 3.8-fold increase at 45°C. Additionally, the primed C was positively correlated with K/r, R/L, and the abundances of chitin degradation genes in week 4. These functions concurred with an increase in the abundance of resource-acquisition strategists such as *Streptomyces* affiliated to Actinobacteria under warming conditions over time. From week 1 to 4, warming induced a distinctive change in glucose-assimilating bacterial community compositions with a particular decrease in the relative abundance of Actinobacteria while an enriched abundance of Chloroflexi. Taken together, warming-triggered change of priming effect depended on alternation of microbiota and metabolic function over time. These findings provide important insights of how warming mediates microbial metabolic use of fresh C and subsequent SOC mineralization, reflecting the positive feedback between soil C emission and climate warming.

Keywords: carbon decomposition, climate change, DNA-SIP, bacterial life strategy, functional genes

Received 27 April 2025; Received in revised form 20 August 2025; Accepted 28 November 2025; Available online 7 January 2026
Yan Gao, E-mail: gaoyan@iga.ac.cn; #Correspondence Jian Jin, E-mail: jinjian29@hotmail.com

© 2026 CAAS. Publishing services by Elsevier B.V. on behalf of KeAi Communications Co. Ltd. This is an open access article under the CC BY-NC-ND license (http://creativecommons.org/licenses/by-nc-nd/4.0/). Peer review under responsibility of Editorial Board of *Journal of Integrative Agriculture*.
doi: 10.1016/j.jia.2026.01.003

1. Introduction

Soil is the largest C stock in terrestrial ecosystems, higher than vegetation and atmospheric C combined (Lehmann and Kleber 2015). Small changes in soil organic C (SOC) may significantly influence the level of global atmospheric CO_2, eventually, contributing to future climate change (Crowther *et al.* 2016). In order to achieve C neutral against climate change, the attempt to increase soil C stock greatly depends on the fresh C input and its effect on native SOC decomposition, known as the priming effect. The magnitude of priming effect could range from 50 to 380% as a result of the native SOC decomposition being stimulated or suppressed in response to fresh C input (Cheng *et al.* 2014; Huo *et al.* 2017).

Global warming, as a dominant feature of climate change, substantially influences the priming effect. A number of studies demonstrated that positive (Creamer *et al.* 2015; Yanni *et al.* 2018; Tao *et al.* 2024), neutral (Ghee *et al.* 2013; Guttières *et al.* 2021) and negative (Dong *et al.* 2022; Li *et al.* 2023; Ding *et al.* 2025) priming effect in response to increased temperature. Microbiome in response to warming is likely to lead to various scenarios of priming effect. A meta-analysis revealed that the warming effect on native SOC mineralization may be limited by the microbial biomass reduction, and then inhibited priming effect (Li *et al.* 2023). More energy is invested to maintain microbial metabolisms under increased temperature and consequently suppress the growth of microbial population (Dong *et al.* 2022). In contrast, the stimulation of priming effect under warming is attributed to the increase in microbial C-use efficiency and change of community composition (Creamer *et al.* 2015). Overall, the influence of increased temperature on the priming effect may greatly depend on soil microbial responses (Billings and Ballantyne 2013; Tao *et al.* 2024).

In recent years, bacterial and fungal community structures have been recognized to be associated with priming effect in response to warming (Creamer *et al.* 2015; Chen *et al.* 2021). Creamer *et al.* (2015) demonstrated that the warming-induced increase in priming effect (from 12°C to 32°C) was related to Gram-positive (G^+) bacterial abundance and activity. Furthermore, Actinobacteria, Chloroflexi, and Firmicutes potentially contributed to the SOC mineralization in response to temperature increase from 15°C to 35°C in farmland soils, and many of those taxa are able to utilize recalcitrant C compounds (Chen *et al.* 2021). Moreover, different temperature regimes led to changes in the relative abundance of specific microbial taxa within the community, which in turn resulted in various patterns of C utilization and different scenarios of the priming effect (Billings and Ballantyne 2013; Fu *et al.* 2025). Therefore, studying changes in microbial functional genes related to C metabolisms can explain how increased temperature regulates the priming effect and provide insights into the microbial preferential SOC sources to be mineralized, contributing to priming effect. Recent evidence on the direct link of the priming effect with microbial functional traits has been reported in forest soils (Ren *et al.* 2022; Zhao *et al.* 2022; Zhou *et al.* 2022). However, these studies demonstrated contradictory results on the response of microbial functional genes to warming, either enriched genes for the degradation of labile C, leading to negative priming effect in forest soils (Ren *et al.* 2022), or the genes for breaking down stable C, especially chitin, lipids, and lignin, predominately driving the positive priming effect (Zhao *et al.* 2022). Apparently, the magnitude of warming impact on the microbial response to exogenous C source likely determines the direction of priming effect, especially for those microbiotas that not only metabolize C, but also become prevalent in warming environments.

Mollisols in Northeast China are experiencing the dilemma of warming under global climate change (Yu and Ma 2022; Dong *et al.* 2023). Over the past 20 years, surface SOC content in Northeast China's Mollisols has continued to decline, following a long-term depletion that reduced it to just 21.3% of initial levels (Tong *et al.* 2017). The stimulation of positive priming effect by warming may contribute to the SOC loss. In recent years, the effect of warming on priming effect in Mollisols has increasingly attracted attention. An incubation experiment showed that exogenous C addition induced a greater priming effect under 25°C than 15°C in a farming Mollisol (You *et al.* 2021). Moreover, the priming effect was especially enhanced in the rhizosphere of soybean under warming conditions (Guo *et al.* 2023). However, the quantification of priming effect under temperature regimes and relevant microbiota responding to C input still remains largely unknown.

To fill this knowledge gap, we applied ^{13}C-labelled glucose into a farming Mollisol under three warming conditions (25°C, 35°C and 45°C) and used stable isotope probing combined with high-throughput sequencing to answer two essential questions. First, how would priming effect respond to warming in the Mollisol? Second, what specific microbiota that metabolize exogenous C are associated with the response pattern of priming effect? This is based on the premise that exogenous C drives shifts in microbial community composition and function, leading to subsequent SOC turnover. We hypothesize that warming amplifies the priming effect by selectively reshaping exogenous C-mobilizing microbial taxa, thereby modulating metabolic pathways towards enhanced degradation of recalcitrant SOC.

2. Materials and methods

2.1. Sampling site description and pre-incubation

Surface soils (0–10 cm) for this study were sampled in September 2020 from a farming field at Hailun County (47.43°N, 126.63°E), Heilongjiang Province, China, where maize–soybean cropping rotation had been practiced for more than six decades. This region is a continental monsoon climate area of temperate zone, with its annual average temperature of 2.1°C and precipitation of 540 mm. The soils were air-dried, homogenized and sieved through a 2-mm mesh after visible plant residues removed. The soils had clay loam texture with pH 5.5, total C 29.3 g kg^{-1} and total N 2.05 g kg^{-1}. The air-dried soil (equivalent to 30 g oven-dried soils) was put into a PVC core with a nylon mesh on the bottom (height: 5 cm, diameter: 3.7 cm). Each PVC core was placed in a 1-L Mason jar together with a vial filled with 10 mL

distilled water. The soil was pre-incubated for three weeks to activate microbial communities, as previous studies have shown that the pre-incubation of moist soils allows microbial communities to stabilize and re-establish their activity, thereby enabling the priming effects (Zhu *et al.* 2022; Zheng *et al.* 2023; Pingthaisong *et al.* 2024). The soil water content was adjusted to 60% field capacity every two days.

2.2. Experimental design and incubation

A four-week incubation experiment was set up with three temperature treatments, i) 25°C, ii) 35°C and iii) 45°C. For each treatment, three soil cores were amended with ^{13}C-glucose, while additional three cores without glucose addition were used as no-glucose controls. Two additional soil cores from each temperature treatment were amended with ^{12}C-glucose and served as non-labelled controls for quality control and the data from these cores were not included in statistical analyses. Three soil cores amended with ^{13}C-glucose were designated for data analyses. After pre-incubation, the soil with glucose addition in each container was maintained at soil moisture content of 60% of field capacity. ^{12}C-glucose or ^{13}C-labelled glucose (10 atom%) was weekly added to soil at 0.5 mg C g^{-1} soil (Xu *et al.* 2019; Zheng *et al.* 2023). The ^{13}C abundance and substrate dosage are sufficient for the successful separation of ^{13}C-DNA, as has been widely demonstrated in previous soil studies (Wang *et al.* 2024; Ren *et al.* 2025). The successful isolation of ^{13}C-DNA reflects the microbial community that instantly metabolizes the exogenous C source, and those ^{13}C-metabolizing microorganisms are considered as C-utilization-efficient taxa. For each non-glucose control, an equal amount of sterile water was added. Another vail with 10 mL of 1 mol L^{-1} NaOH trap was placed in each Mason jar. The alkali trap was harvested and replaced with a new one weekly. Soil cores were destructively sampled at the end of weeks 1, 2 and 4 for subsequent soil and microbial analyses. Each sample was partitioned into three subsamples: ~18 g of fresh soil was used for microbial biomass C and dissolved organic C measurements; ~2 g was stored at –80°C for DNA extraction and sequencing; the remainder was air-dried for chemical property analysis.

2.3. CO_2 flux and priming effect quantification

The total CO_2 emissions were quantified with the titration method. Briefly, 2 mL of NaOH trap solution was mixed with 6 mL of 0.25 mol L^{-1} $SrCl_2$ for precipitation reaction. Then, 0.1 mol L^{-1} HCl was used to titrate excessive NaOH with 1% phenolphthalein as an indicator. The consumed amount of HCl solution was used to calculate total CO_2 emissions. To differentiate glucose- and SOC-derived CO_2 sources, an aliquot from the alkali traps was treated with $SrCl_2$ to form a $SrCO_3$ precipitate suspension. The suspension pH was adjusted to 7.0 prior to further processing. The precipitates collected during week 1 (days 0–7) and week 4 (days 21–28) were washed three times with deionized water. After oven-dried at 60°C for 48 h, the precipitates were subjected to ^{13}C abundance measurement using Isotope Ratio Mass Spectrometer (Sercon 20-22, Gateway, Crewe, UK).

2.4. Biochemical analyses

Soil pH was determined by a pre-calibrated pH meter (soil:water ratio of 1:5). Microbial biomass C (MBC) and N (MBN) were assessed by the chloroform fumigation-extraction method (Vance *et al.* 1987). Total organic C and total N in the fumigated and unfumigated extractions were measured using a TOC/TN analyzer (multi N/C 3100, Analytik Jena, Jena, FT, Germany). The MBC and MBN were calculated as the difference of total organic C and total N in the extracts of fumigated and unfumigated soil samples, and they were adjusted by conversion factors of 0.45 and 0.54, respectively (Jenkinson *et al.* 2004). Soil dissolved C (DOC) and dissolved total N (DTN) were equivalent to total organic C and total N in unfumigated samples. Microbial metabolic quotient (qCO_2) was calculated from total CO_2 release divided by MBC at the end of each week (Zheng *et al.* 2023).

2.5. Data collection for the response of microbial community in warming incubations

To overview the general response of bacterial community to increased temperatures, we conducted a meta-analysis on research papers published in peer-reviewed journals between 2015 and 2024. The details of studies used in the meta-analysis are provided in Appendix A. We searched Web of Science databases with terms of “warming”, “elevated temperature”, “incubation”, “temperature sensitivity”, “bacteria”, “microbial community”, “16S”, “high-throughput sequencing”, and “Illumina” targeting titles, keywords, and abstracts. Here, we included amplicon-based high-throughput sequencing data, a widely recognized method in microbial community studies. We also performed the analysis on the bacterial communities at the phylum and genus levels, as these taxonomic levels were most frequently reported in the literature. For each study, we compiled data on the impact of warming on standard microbial α-diversity indices (Z-score), including Pielou’s evenness, richness, Shannon, and abundance-based coverage estimator (ACE) indices. To visually compare microbial compositions between treatments, we carried out non-metric multidimensional scaling (NMDS) analysis using the *metaMDS* function in *vegan* package of R. Additionally, to assess the significance of warming influence on bacterial community composition, we conducted a forward permutational multivariate analysis of variance (PERMANOVA) with 999 permutations, utilizing the adonis function in the vegan package. The treatment group was categorized into four temperature groups, i.e., 15°C, 25°C, 35°C and 45°C. To ensure data precision and quality, we filtered out the taxa with an average relative abundance below 1%, thereby excluding those with low abundance. We omitted data for any taxa that were absent in any treatment or replicate within a study, following the methodology of Zhao *et al.* (2024).

2.6. DNA extraction and SIP

Total DNA was extracted from each of the five replicated soil samples (0.5 g fresh weight per replicate) using the FastDNA Spin Kit for Soil (MP Biomedicals, USA). DNA concentrations from all extracts were quantified using a Qubit™ 4 fluorometer

(Thermo Fisher Scientific, Waltham, MA, USA), and samples were stored at –20°C until subsequent analysis.

Regarding the SIP procedure, in turn, 4.9 mL CsCl (1.85 g mL^{-1}), 0.9 mL gradient buffer (GB) and 100 μL total GB containing 4.0 μg soil DNA were added to each 15-mL centrifuge tube and mixed to reach a buoyant density of 1.4029±0.0002 measured by the refractometer (Atago, Pacifico Energy, Tokyo Stock Exchange, Japan). The solution was transferred into a sealed polyallomer centrifuge tube (Beckman Coulter, Brea, CA, USA) using a cordless tube topper and centrifuged at 179,000×g and 20°C for 44 h on a Vti 65.2 rotor in an Optima L-XP ultracentrifuge (Beckman Coulter, Brea, CA, USA). The solution in each centrifuged tube was divided into 15 fractions with a syringe pump. The buoyant density of each fraction was determined by the refractometer. The DNA fractions corresponding to the heavier density range with a buoyant density ≥1.71 or 1.72 g mL^{-1} were designated as glucose-incorporated DNA. Here, the observed inconsistency in buoyant densities resulted from conducting ultracentrifugation in separate batches, leading to minor shifts in the buoyant density of the ^{13}C-DNA fraction. DNA fractions with buoyant densities <1.71 or 1.72 g mL^{-1} were classified as non-glucose-incorporated (light) DNA, i.e., ^{12}C-DNA fraction and subsequently included in sequencing analyses. Then, 550 μL of PEG 6000 solution was added to each buoyancy density fraction to precipitate DNA at room temperature for 2 h. The DNA precipitate was washed with 70% ethanol and dried for 15 min before resuspended in 30 μL TE buffer. Subsequently, qPCR was used to measure the abundance of the 16S rRNA gene in each fraction. The PCR amplification, DNA sequencing and SIP validation are further detailed in Appendix B. Using PCoA and DESeq2, the heavier fractions with the highest 16S rRNA gene abundance of ^{13}C-DNA was statistically compared with the light fractions from the ^{12}C-DNA control, allowing the identification of glucose-metabolizing microbes (see in Appendices C and D).

2.7. Evaluations of K- and r-strategy groups ratio

Here, we define copiotrophic and oligotrophic taxa, as well as r- and K-strategy groups as representatives of a continuum within bacterial populations, and treat those classifications as heuristic categories rather than a strict dichotomy (Fierer *et al.* 2007; Li *et al.* 2021). Based on the sequencing results and previously published studies (Li *et al.* 2021; Ma *et al.* 2023), a detailed delineation of bacterial taxa assigned to K- and r-strategy groups is presented in Appendix E. The ratio of K- to r-strategists (K/r) within the microbial community was calculated by aggregating the relative abundances of taxa recognized or hypothesized to exhibit K- or r-strategic behaviors. Our designation of K- and r-strategists for bacterial taxa aligns broadly with findings from previous studies (Li *et al.* 2021; Ma *et al.* 2023).

Alpha-Proteobacteria, Planctomycetes, and Acidobacteria are identified as relative K-strategists (oligotrophs) due to their ability to metabolize more resistant organic matters such as hemicellulose or cellulose (Ali *et al.* 2018; Razanamalala *et al.* 2018). Chloroflexi is also identified as a relative K-strategist, characterized by their slow growth rates (Davis *et al.* 2011), and is typically found in nutrient-deficient environments. Gamma-Proteobacteria are known for their rapid growth as copiotrophic organisms, thriving on labile organic substrates, and are thus considered typical r-strategists (copiotrophs; Fierer *et al.* 2007; Eilers *et al.* 2010; Liang *et al.* 2024).

2.8. Functional prediction and calculation of recalcitrant and labile C degrading gene ratio

PICRUSt2 is widely used in the field of function prediction based on amplicon sequences (Douglas *et al.* 2019). In this study, PICRUSt2 was employed to explore the potential effects of different temperature conditions on microbial functions. The annotation of pathways and enzymes or genes was based on the Kyoto Encyclopedia of Genes and Genomes (KEGG) database and Enzyme Commission (EC) numbers. Specifically, the abundances of microbial functions, enzymes, and genes were obtained by analyzing the 16S rRNA gene sequences using PICRUSt2. Subsequently, enzymes and genes with abundances higher than 0.5% that were involved in the degradation of recalcitrant and labile C were screened out and listed in Appendix F. Recalcitrant C/labile C gene ratio (R/L) was calculated for each sample as follows: The abundance of all recalcitrant carbon-degrading genes and the abundance of all labile carbon-degrading genes were summed separately to obtain the R value and the L value, respectively. The R value was then divided by the L value. And the R/L gene ratios were compared at 25°C, 35°C and 45°C at weeks 1 (day 7) and 4 (day 28). The significance level was set at $P<0.05$.

2.9. Calculation and statistical analysis

In the glucose-added treatments, glucose-derived and SOC-derived CO_2 fluxes were estimated as follows (Fontaine *et al.* 2004; Zhu *et al.* 2022; Tian *et al.* 2023):

$$Glu_CO_2=CO_2\ flux\times\left(\frac{AT\%_{glu\text{-}amended}-AT\%_{ck}}{AT\%_{glu}-AT\%_{ck}}\right) \quad (1)$$

$$SOC_CO_2=CO_2\ flux-Glu_CO_2 \quad (2)$$

where Glu_CO_2, SOC_CO_2 and CO_2 flux represent CO_2 emissions from glucose, SOC and total CO_2 in glucose-supplied soils, respectively; $AT\%_{ck}$ and $AT\%_{glu\text{-}amended}$ are the ^{13}C atom% of CO_2 in the control and glucose-amended soils, respectively; $AT\%_{glu}$ represents the ^{13}C atom% of the added glucose-C.

The primed C was calculated by SOC-derived CO_2 minus CO_2 flux in the no-glucose control as the following equation:

$$Primed\ C=SOC_CO_2-CK_CO_2 \quad (3)$$

Data analyses were carried out using the R platform (version 4.0.3). One-way analysis of variance (ANOVA) was performed to assess the effect of different temperature conditions on CO_2 flux, glucose-derived CO_2 flux, primed C, soil properties and the glucose-assimilating bacterial α-diversity indices. The differences in the 16S rRNA gene sequencing in heavy fractions for ^{13}C-DNA and light fractions for ^{12}C-DNA were assessed by Differential Expression Sequencing 2 (DESeq2). Principal co-ordinate analysis (PCoA) was employed to visualize the structural orientation of glucose-assimilating bacterial community.

The PERMANOVA was adopted to assess the effect of temperature and incubation time on glucose-assimilating bacteria community structures. The association between soil properties and the relative abundance of microbial functional genes, and between the relative abundances of K-strategists or r-strategists and priming effect were evaluated based on Spearman's correlation test using the "corr.test" function within the psych package.

We hypothesized that warming could lead to changes in soil C utilization and metabolic processes, prompting microbial adaptations through structural and functional changes, potentially impacting priming effect. To assess the impact of elevated temperature on priming effect, we utilized the partial least squares path model (PLS-PM) in the package plspm, considering different temperatures as an external factor and soil properties, microbial biomass, diversity, structural and functional characteristics as internal variables. We initially conducted a PLS-PM to identify and eliminate variables with loadings below 0.7. Subsequently, we refined the model with the remaining variables (Wang *et al.* 2016). The relationships between these key variables were quantified using path coefficients. To assess the predictive accuracy of our models, we employed the goodness of fit (GoF) index. We chose PLS-PM for its flexibility with sample size, robust statistical power, and ability to provide solutions when other methods fail (Ali *et al.* 2017; Zhong *et al.* 2020).

3. Results

3.1. Impact of warming on priming effect and associated biochemical properties

Increasing temperature inhibited the priming effect in week 1 but stimulated the positive priming effect with 3.8 times increase at 45°C compared with the control in week 4 (Fig. 1-A; $P<0.05$), contributing to a significant temperature by time interaction. Increasing temperature increased soil respiration and glucose-derived CO_2 (Fig. 1-B and C; $P<0.05$). In week 1, the respiration rate at 25°C was 410 mg C kg^{-1}, 15 and 23% lower than those at 35°C and 45°C. The same trend was found in week 4 (Fig. 1-B). Similarly, warming also resulted in the significant increase in glucose-derived CO_2 (Fig. 1-C; $P<0.05$). Additionally, compared to the control, microbial respiration quotient was significantly increased concurrently at 45°C in both weeks 1 and 4 (Fig. 1-D; $P<0.05$).

Warming significantly increased the concentrations of DOC and DTN in soil in weeks 1 and 4 (Fig. 2-A and B; $P<0.05$), but decreased the DOC/DTN ratio in week 4 (Fig. 2-C; $P<0.05$). Warming significantly decreased soil MBC and MBN concentrations and MBC/MBN in week 4 (Fig. 2-D–F; $P<0.05$).

3.2. Universal impact of warming on soil bacterial community diversity: A meta-analysis

The meta-analysis indicates the significant decrease of α-diversity of soil bacterial community in response to the increase of temperature, including species richness, Shannon and ACE indices (Fig. 3-A–D). With the meta-analyses incorporating the sequencing data from different farming systems, a universal finding was that increasing temperature significantly influenced bacterial community compositions in soils as indicated by NMDS (Fig. 3-E). Specifically, community similarity analysis highlighted significant variation of bacterial community composition under different temperature regimes in each soil (Appendix G).

In addition, the meta-analysis indicated that Actinobacteria and Chloroflexi phyla had greater abundances under warming conditions (Fig. 4-A; $P<0.05$), as reflected with a significant increase in the abundances of *Nocardioides* and *Streptomyces* (Fig. 4-B; $P<0.05$). In contrast, Proteobacteria and Acidobacteriota were less prevalent under 45°C (Fig. 4-A; $P<0.05$).

3.3. Warming effect on glucose-assimilating bacterial community diversity and functions

Alpha-diversity indices of the glucose-assimilating bacterial community (^{13}C fraction) were lower under warming conditions compared to the control (Fig. 5-A–D). For the glucose-assimilating bacterial communities, PCoA and PERMANOVA analysis revealed a distinct clustering of bacterial community in response to warming and incubation time, with particularly pronounced differences in community composition at 45°C compared to 25 and 35°C in week 4 (Fig. 5-E).

Actinobacteria were enriched under warming in week 1 while no significant change in week 4 (Fig. 5-F). However, warming decreased the abundance of Proteobacteria in

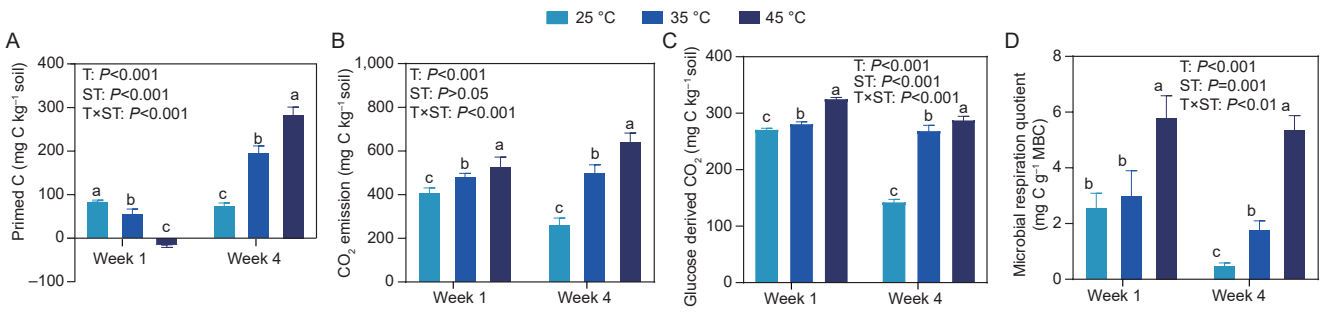


Fig. 1 Primed C (A), total CO_2 emissions (B), glucose-derived CO_2 (C) and microbial respiration quotient (D) under temperatures of 25°C, 35°C and 45°C for the week 1 (days 0–7) and 4 (days 21–28). T, temperature; ST, sampling time. Data are the mean±standard errors. Different lowercase letters indicate significant differences ($P<0.05$) between treatments at the same sampling time.

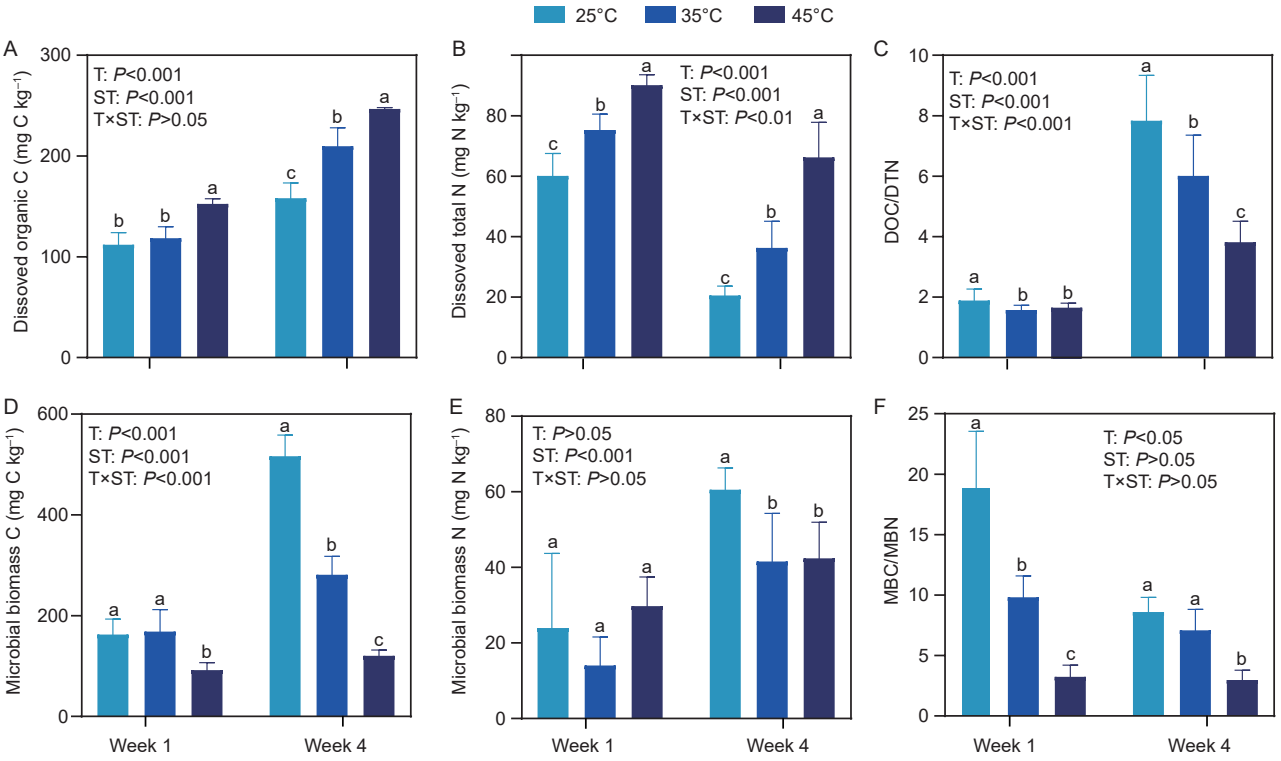


Fig. 2 Dissolved organic C (DOC) (A), dissolved total N (DTN) (B), DOC/DTN ratio (C), microbial biomass C (MBC) (D), microbial biomass N (MBN) (E), MBC/MBN ratio (F) under 25°C, 35°C and 45°C at weeks 1 (day 7) and 4 (day 28). T, temperature; ST, sampling time. Data are the mean±standard errors (n=3). Different lowercase letters indicate significant differences (P<0.05) between treatments at the same sampling time.

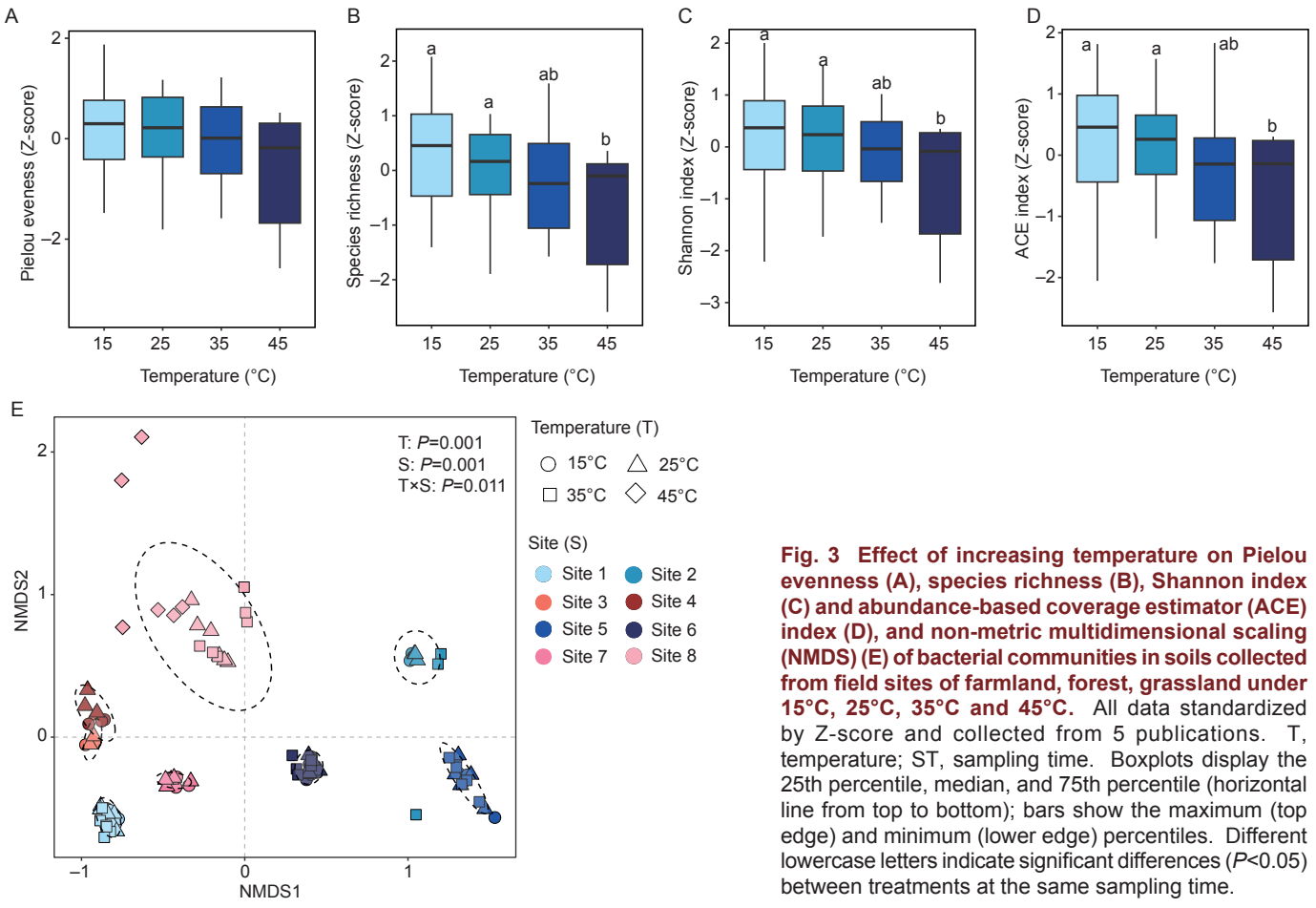


Fig. 3 Effect of increasing temperature on Pielou evenness (A), species richness (B), Shannon index (C) and abundance-based coverage estimator (ACE) index (D), and non-metric multidimensional scaling (NMDS) (E) of bacterial communities in soils collected from field sites of farmland, forest, grassland under 15°C, 25°C, 35°C and 45°C. All data standardized by Z-score and collected from 5 publications. T, temperature; ST, sampling time. Boxplots display the 25th percentile, median, and 75th percentile (horizontal line from top to bottom); bars show the maximum (top edge) and minimum (lower edge) percentiles. Different lowercase letters indicate significant differences (P<0.05) between treatments at the same sampling time.

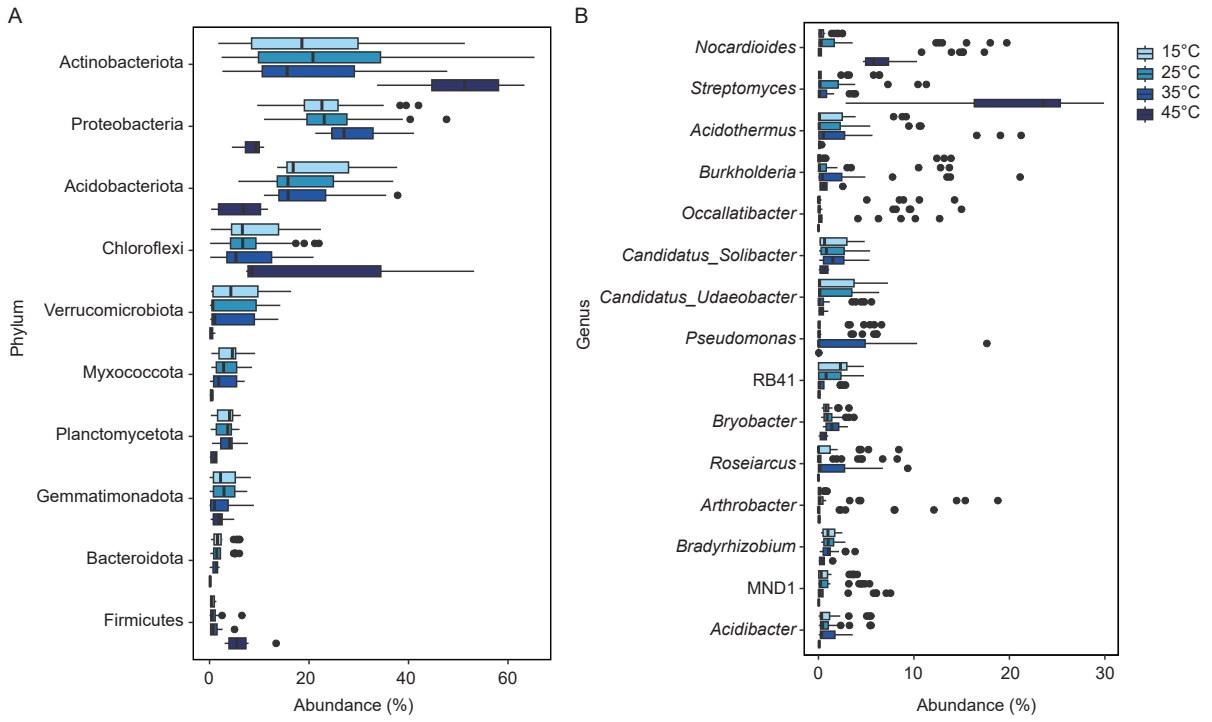


Fig. 4 Effects of increasing temperature on the relative abundance of dominant phyla (A) and genera (B). All data collected from 5 publications. Boxplots display the 25th percentile, median, and 75th percentile (horizontal line from top to bottom), and bars show the maximum (top edge) and minimum (lower edge) percentiles.

week 1. It significantly decreased the abundance of glucose-assimilating Acidobacteriota in week 1 but increased that of Chloroflexi in week 4 (Fig. 5-F; $P<0.05$). At the genus level, increasing temperature from 25°C to 45°C significantly increased the abundance of *Streptomyces* but decreased the abundances of *Nocardioides*, *Arthrobacter*, and *Burkholderia* at weeks 1 and 4 (Fig. 5-G; $P<0.05$).

In week 1, the K/r was notably lower at 35°C and 45°C compared to 25°C. However, in week 4, warming significantly increased such a ratio (Fig. 6-A; $P<0.05$). The trend of R/L was similar to the K/r in both weeks 1 and 4 but warming increased the R/L at week 4, especially at 45°C (Fig. 6-B; $P<0.05$).

3.4. Associations of microbial taxa and functions with priming effect

Some microbial taxa demonstrated similar dynamic patterns with priming effect, resulting in significant correlations between the priming effect and the relative abundances of *Nocardioides*, *Streptomyces*, *Arthrobacter*, *Amycolatopsis*, and *Gemmatimonas* in both weeks, with positive correlations between priming effect and *Streptomyces* in week 4 (Fig. 7-A–E; $P<0.05$).

The PLS-PMs demonstrated the association of variables with the priming effect, as these variables explained 86.6 and 83.3% of the priming effect variation for weeks 1 and 4, respectively, and had a robust fit to it for each sampling time with a GoF value exceeding 0.68 (Fig. 8-A and B). The standardized total effects in PLS-PM revealed that K/r-strategist ratio, C metabolism, and α-diversity positively influenced the priming effect in week 1, with the direct effect of α-diversity and indirect effect of labile C availability (DOC), and C metabolism (MBC and qCO_2) (Fig. 8-C). In week 4, the C availability still posed a significant indirect effect on the priming effect through the K/r-strategist ratio (Fig. 8-B). The positive effect of K/r-strategist ratio on the priming effect was the greatest among the standardized total effects (Fig. 8-D).

4. Discussion

4.1. Warming-induced priming effect differs over time

During week 1, the negative priming effect at 45°C (Fig. 1-A) demonstrated that soil microorganisms preferentially consumed readily available glucose over native SOC. The negative priming effect is likely because the increased proportion of rapid growth strategies (r-strategists) preferentially used available substrates. Many r-strategists (copiotrophs) have higher respiration rates than K-strategists (oligotrophs) (Fanin *et al.* 2020; Chen *et al.* 2021), contributing to the increased CO_2 efflux in response to warming (45°C). The decrease of the K/r (Fig. 6-A) likely led to the acceleration of the energy flux through the copiotrophic channel under warming conditions. Moreover, when soil N is enriched (indicated by rise in DTN, Fig. 2-B), these fast-growing microbes opt for the added glucose over SOC to meet their C and energy demands, thus inhibiting SOC decomposition (Kuzyakov 2010; Huang *et al.* 2024). Our results are supported by the previous theory of "preferential substrate utilization", contributing to a negative priming effect (Blagodatskaya and Kuzyakov 2008). This is also evidenced by a higher microbial respiration quotient (qCO_2) and a more

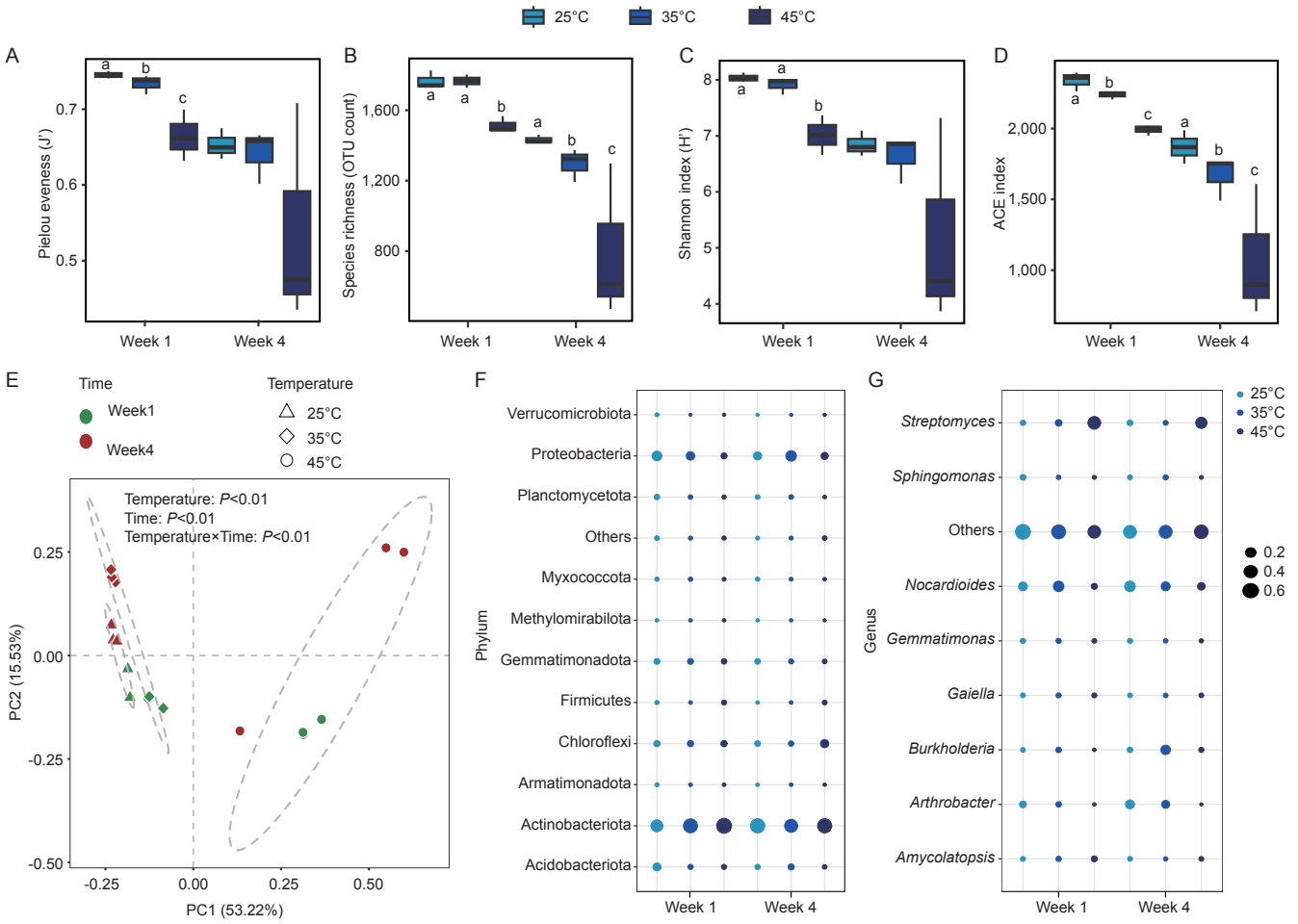


Fig. 5 Effects of increasing temperature on Pielou evenness (A), species richness (B), Shannon index (C) and abundance-based coverage estimator (ACE) index (D), principal coordinate analysis (PCoA) (E) and the relative abundance of dominant phyla (F) and genera (G) of glucose-assimilating bacterial community under temperature treatments of 25°C, 35°C and 45°C at weeks 1 and 4. Boxplots display the 25th percentile, median, and 75th percentile (horizontal line from top to bottom), and bars show the maximum (top edge) and minimum (lower edge) percentiles. Different lowercase letters indicate significant differences (P<0.05) between treatments at the same sampling time.

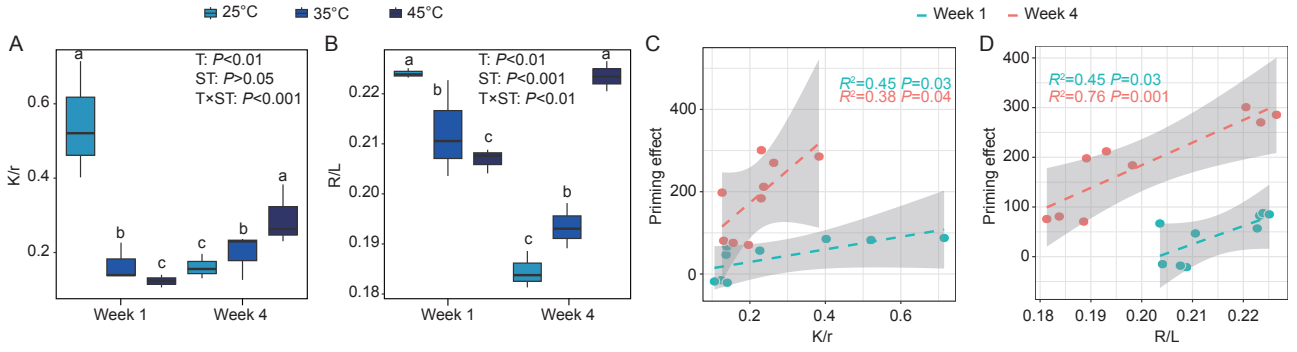


Fig. 6 The K/r-strategists ratio (K/r) (A), recalcitrant/labile C gene ratio (R/L) (B), and relationships of the priming effects with the K/r-strategists ratio (C) and R/L gene ratio (D) under temperatures of 25, 35 and 45°C at weeks 1 and 4. T, temperature; ST, sampling time. Boxplots display the 25th percentile, median, and 75th percentile (horizontal line from top to bottom), and bars show the maximum (top edge) and minimum (lower edge) percentiles. Different lowercase letters indicate significant differences (P<0.05) between treatments at the same sampling time. Significant relationships are shown with dashed lines (P<0.05), while grey areas are the 95% confidence intervals of these models.

substantial increase in total CO_2 and glucose-derived CO_2 emissions at 45°C (Fig. 1).

The positive priming effect at 25°C and 35°C in week 1 might stem from N limitation relative to the labile C inputs.

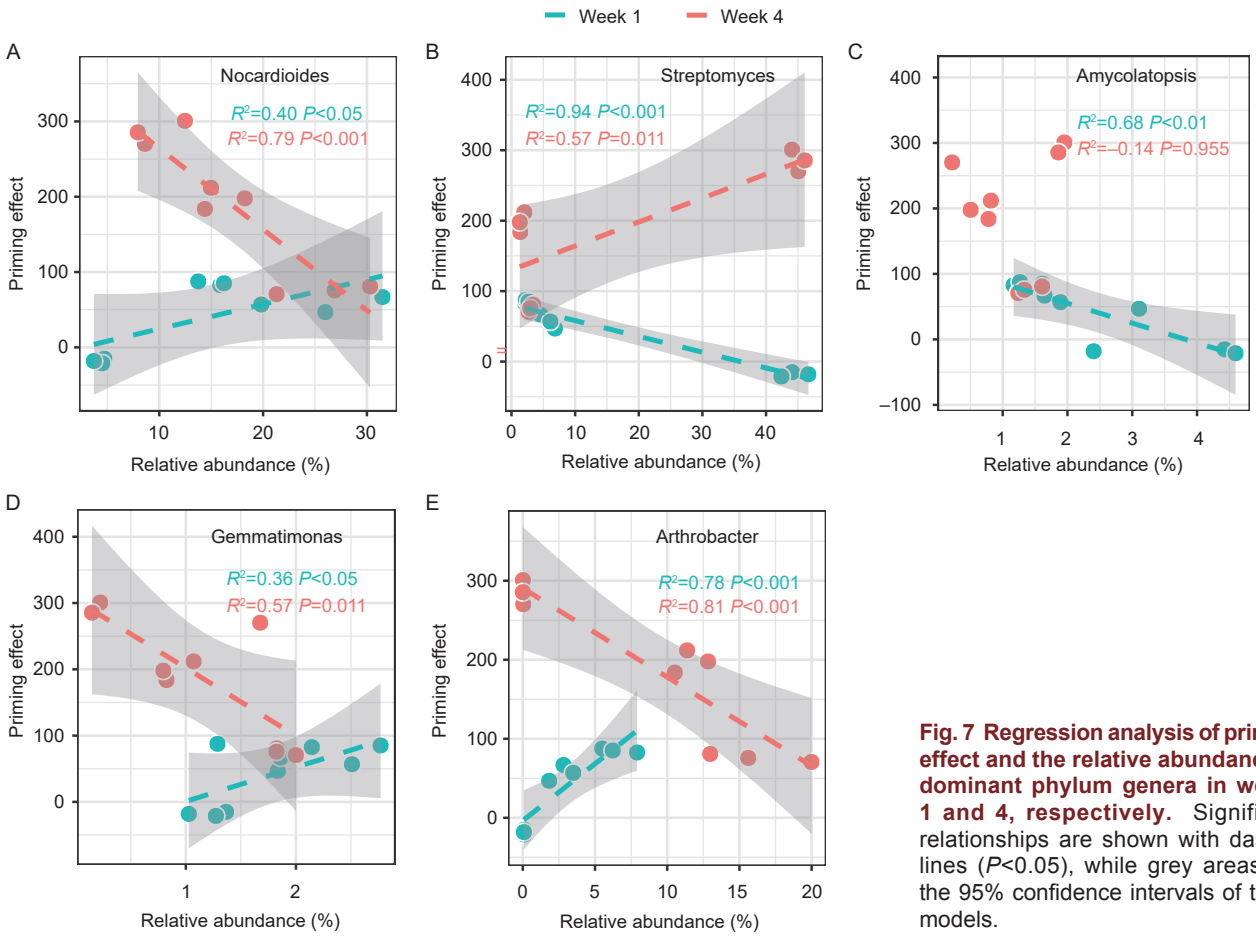


Fig. 7 Regression analysis of priming effect and the relative abundance of dominant phylum genera in weeks 1 and 4, respectively. Significant relationships are shown with dashed lines (P<0.05), while grey areas are the 95% confidence intervals of these models.

Microbial growth spurred by available C lowered the mineral N in soil. To counteract N scarcity, microorganisms resort to decomposing N-rich, recalcitrant organic matters to acquire N, which is "microbial N-mining" theory (Pausch *et al.* 2024; Reji *et al.* 2024). However, the comparatively weaker priming effect observed after glucose addition at 35°C compared to 25°C in week 1 (Fig. 1-A) indicates that warming alleviates microbial N limitation on their growth (Li *et al.* 2018; Cui *et al.* 2020), as evidenced by reduction in the DOC/DTN ratio (Fig. 2-C), thereby reducing the priming effect in soil. This explanation is supported by our observation of a significant increase in DTN concentration (Fig. 2-B) at 35°C compared to 25°C. Furthermore, Cui *et al.* (2024) demonstrated that increasing temperature from 25°C to 35°C reduced the microbial N demand, accompanied by lower activities of N-acquiring enzymes, and coincided with the suppression of priming effect. In the present study, warming decreased the MBC/MBN ratio (Fig. 2-F), suggesting that microorganisms adapted to higher temperatures were less N-deficient. Consequently, warming-induced positive priming effect due to "microbial N mining" was weaker during initial incubation time. The significant negative correlation between the changes in DTN and the priming effect indicates that an increase in microbial demand for DTN enhances the mineralization of soil organic matter. To further test this hypothesis, dual $^{15}N/^{13}C$ isotopic labelling is needed to trace the influence of N availability on microbial N-mining strategies associated with the priming effect.

After a 4-week incubation, the higher positive priming effect at 45°C than 25°C (Fig. 1-A) indicates the stronger microbial contribution to the priming effect in response to high temperature. Although the decreases of the DOC/DTN and MBC/MBN ratios under warming (Fig. 2-C and F) were positively associated with the stimulation of the priming effect, fitting the microbial stoichiometric homeostasis theory, increasing temperature markedly decreased MBC. This implies that stoichiometric theory does not apply to this positive priming effect. Given that the adaptation of microbial communities to the soil C/N ratio may not play a role in SOC decomposition (Song *et al.* 2022), the microbial community in this study shifted over time towards the metabolic preference to mineralization of soil organic matter under warming (Cheng *et al.* 2014; Feng *et al.* 2021). The marked increase in the abundance of chitin-degradation genes under warming conditions by week 4 (Appendix H-a) suggests a catabolic potential for chitin breakdown. The C in chitin, partially derived from SOC, may contribute to the increased priming effect under warming conditions, especially 45°C. This viewpoint is further evidenced by the positive correlations between priming effect and abundances of chitin-degradation genes (Appendix H-b). Furthermore, the recycle of microbial necromass, comprising of chitin, supports the increase in glucose-derived CO_2 and SOC-derived CO_2 emissions, as the necromass was predominantly sourced from the added glucose.

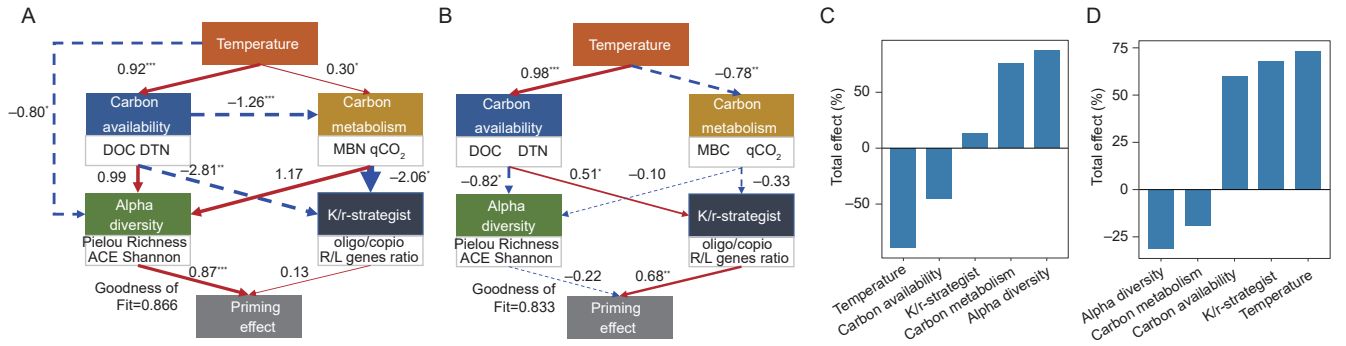


Fig. 8 Partial least squares path model (PLS-PM) assessing the influence of increased temperature on soil priming effect through various pathways (A and B), and the standardized total effects (direct plus indirect effects) of temperature, C availability, C metabolism, α-diversity and K/r-strategist ratio in PLS-PM on the primed C at week 1 (C) and 4 (D). DOC and DTN represent dissolved organic C and dissolved total N, respectively; MBC, MBN, and qCO_2 represent microbial biomass C and N, and microbial metabolic quotient, respectively, while Pielou, Richness, ACE and Shannon indicate Pielou evenness, Species richness, Shannon index and ACE index, respectively, and oligo/copio and R/L gene ratio indicate the ratio of relative abundances of oligotrophs to copiotrophs and the ratio of recalcitrant C to labile C genes, respectively. Path coefficients that differed significantly were indicated by * (P<0.05), ** (P<0.01) and *** (P<0.001).

4.2. Microbial attributes to priming effect

Bacterial diversity could be associated with warming-induced decrease of priming effect in week 1 as the PLS-PM analysis revealed a strong positive link between bacterial α-diversity and priming effect (Fig. 8-A). Typically, a lower α-diversity results in reduced ecosystem functional redundancy and insufficient functional complementarity (Wagg *et al.* 2019; Li *et al.* 2024). Our results align with previous research and demonstrate that soil with low bacterial diversity significantly restricts SOC decomposition (Karimi *et al.* 2017; Wagg *et al.* 2019; Yu *et al.* 2020). Moreover, the decrease in bacterial diversity under warming may also diminish the functional response in SOC decomposition (Hou *et al.* 2025). A possible explanation for the linkage between bacterial diversity and priming effect is that the bacterial community with a low diversity had reduced metabolic potential to decompose a large spectrum of complex C compounds (Baumann *et al.* 2013; Zhang *et al.* 2024), and thus the priming effect in soil. This result was also supported by the decreases in the K/r and R/L ratios under the warming condition in week 1 (Fig. 6-C and D) because K-strategists normally secrete more oxidases and N-acquired enzymes than r-strategists for breaking down complex organic matter to acquire the required N (Cui *et al.* 2024). However, an opposite trend of priming effect under warming applied in week 4, indicating that the microbial metabolic functions were enhanced in terms of decomposition of complex organic compounds.

Thus, bacterial diversity may not be the major contributor to the priming effect variation over time under warming. Indeed, the change in bacterial community composition explained the variations in the priming effect. A distinct clustering of glucose-assimilating bacterial community at 45°C compared to 25°C and 35°C in week 4 in this study (Fig. 5-E) indicates that warming may select microbial communities with a stronger capacity to decompose native SOC, which was confirmed by the change in relative abundance of microbial taxa (Fig. 5-F and G). Moreover, warming accelerated the temporal succession of bacterial community compositions, especially K-strategists that preferentially utilize recalcitrant organic matter (Li *et al.* 2021; Lyu *et al.* 2025). For example, warming induced a marked decrease in the relative abundance of Actinobacteria while Chloroflexi became enriched from week 1 to 4 (Fig. 5-F), indicating that K-strategists gradually dominated the microbial communities over time under warming. The growing dominance of K-strategists may be due to the increased mortality of r-strategists under warmer conditions, rather than a direct increase in the population of K-strategists (Cui *et al.* 2024). Moreover, a greater loss of MBC and MBN at 45°C compared to 25°C in week 4, is likely due to the increased mortality rate of r-strategists (Kaiser *et al.* 2014).

Given that the bacteria here assimilated glucose and were dominantly K-strategists under warming by week 4, these microbial taxa were likely to consume necromass from previous microbial generations. Microbial turnover, death and the subsequent generation of necromass are primarily attributed to r-strategists (Kaiser *et al.* 2014; Zhou *et al.* 2024), whose cellular components contribute significantly to the necromass pool (Liang *et al.* 2019). These K-strategists predominantly consume the necromass of r-strategists to obtain energy and nutrients due to the compositional (low C/N ratio and easily decomposed) (Paul 2007; Cui *et al.* 2018) and physical advantages of the necromass (not tightly bound to the soil mineral phase, and located in places already occupied by living microorganisms) (Kuzyakov and Mason-Jones 2018). Furthermore, we extended the K/r selection theory to encompass functional gene data in response to warming, aiming to elucidate the link between primed C values and C-degradation genes. By conducting phospholipid fatty acid (PLFA) analysis, previous studies have also demonstrated a strong connection between soil priming effect and the presence of microbial K-strategists (Cui *et al.* 2024). In addition, Liang *et al.* (2024) reported that the microbial community shifted from r- to K-strategists due to the exhaustion of labile resources resulted in microbial C limitation at a later stage of straw decomposition, the

dominant K-strategist bacteria increased the decomposition of recalcitrant SOC for energy and nutrients, resulting in a positive priming effect. Given that K-strategists adapt to nutrient-poor environments and are efficient at mineralizing recalcitrant C, their dominance likely underpins the enhanced priming effect under warming conditions. Notably, the priming effect rose with an increase in the ratio of bacterial K- to r-strategists (Fig. 6-C) and genes involved in the degradation of recalcitrant over labile C (Fig. 6-D), suggesting that fresh C inputs stimulate the loss of native SOC by increasing the abundance of microbial genes responsible for recalcitrant C decomposition. The results are consistent with those of a previous study (Zhao *et al.* 2022) which revealed a robust positive correlation between the prevalence of microbial C decomposition genes and priming effect, and the microbial functional genes responsible for the increased priming effect *via* decomposition of stable C compounds (such as lignin, lipids, and chitin). However, in this study, the shift of bacterial community from r- to K-strategists with the increase of temperature may be associated with microbial community adaptability to high temperature even though the increased DOC and DTN under warming did not thrive the r-strategists (Fig. 2-A and B). This is supported by previous studies showing the adaptation of a wide range of K-strategists to abiotic stresses including high temperature (Fierer *et al.* 2007; Cui *et al.* 2024).

In the community, a number of keystone taxa may primarily contribute to the priming effect in response to warming. We showed that the abundance of *Nocardioides* (branch of Actinobacteria) had a negative correlation with primed C (Fig. 7-A). *Nocardioides* belongs to r-strategists, and mainly degrades the labile C rather than enhancing SOC. In addition, we also found that *Arthrobacter* (branch of Actinobacteria) was negatively correlated with primed C in week 4 (Fig. 7-E). Actinobacteria were able to grow preferentially on the C-rich refractory materials and relatively easily decompose the cellulose and lignocellulose (Khodadad *et al.* 2011), indicating that these microorganisms preferentially use the C source that is used partially by others. Additionally, the genus *Streptomyces* that was positively correlated with primed C in week 4 in this study (Fig. 7-B), was closely associated with litter decomposition and SOC mineralization (Zhang *et al.* 2024). *Streptomyces* is among the identified bacteria capable of degrading more recalcitrant C fractions, such as lignin and chitin (Tan *et al.* 2022; Duhsaki *et al.* 2023) although it is one of the copiotrophic bacterial groups (Fang *et al.* 2022) and preferentially uses labile C sources owing to their higher growth efficiency (Fierer *et al.* 2007; Eilers *et al.* 2010). Our study further confirms that *Streptomyces* could degrade recalcitrant soil C through co-metabolic processes towards the end of incubation. Consequently, the priming effect may be enhanced by enriched *Streptomyces* genus under warming.

5. Conclusion

Warming-induced reverse change in the priming effect could potentially be attributed to the evolution of microbial metabolic functions over time. With exogenous C input, warming initially accelerated the energy flux through r-strategists. The increased proportion of r-strategists opt for the exogenous C over SOC to meet their C and energy demands, resulting in a decreased priming effect. Over time, however, the abiotic stress-resistant K-strategists become prevalent in the exogenous-C-metabolizing community under warming, which were responsible for recalcitrant SOC decomposition and intensified positive priming effect. Overall, our findings advance our knowledge of specific role of K-strategists in the positive feedback between soil C emission and climate warming. Although our research on laboratory incubation constitutes a mere fragment of a vast and complex system, the findings offer crucial insights into understanding soil C dynamics in a world of warming and contribute significantly to the improvement of models to predict soil C stocks under warming climate scenarios. Future research endeavors should assess the microbial trophic strategies relevant to the priming effect in broader geographic scales.

Acknowledgements

The project was funded by the International Partnership Program of Chinese Academy of Sciences (131323KYS B20210004), the Strategic Priority Research Program of Chinese Academy of Sciences (XDA28020201), the National Key R&D Program of China (2021YFD1500400), and the Key Program of Natural Science Foundation of Heilongjiang Province, China (ZD2021D001).

Declaration of competing interest

The authors declare that they have no conflict of interest.

Declaration of generative AI and AI-assisted technologies in scientific writing

The authors declare that they did not use AI in the preparation and writing of this manuscript.

Appendices associated with this paper are available at https://doi.org/10.1016/j.jia.2026.01.003

References

Ali H E, Reineking B, Münkemüller T. 2017. Effects of plant functional traits on soil stability: Intraspecific variability matters. *Plant and Soil*, **411**, 359–375.

Ali R S, Poll C, Kandeler E. 2018. Dynamics of soil respiration and microbial communities: Interactive controls of temperature and substrate quality. *Soil Biology and Biochemistry*, **127**, 60–70.

Baumann K, Sanaullah M, Chabbi A, Dignac M F, Bardoux G, Steffens M, Kögel Knabner I, Rumpel C. 2013. Changes in litter chemistry and soil lignin signature during decomposition and stabilisation of ^{13}C labelled wheat roots in three subsoil horizons. *Soil Biology and Biochemistry*, **67**, 55–61.

Billings S A, Ballantyne I F. 2013. How interactions between microbial resource demands, soil organic matter stoichiometry, and substrate reactivity determine the direction and magnitude of soil respiratory responses to warming. *Global Change Biology*, **19**, 90–102.

Blagodatskaya E, Kuzyakov Y. 2008. Mechanisms of real and apparent priming effects and their dependence on soil microbial biomass and community structure: Critical review. *Biology and Fertility of Soils*, **45**, 115–131.

Chen G, Fang Y, van Zwieten L, Xuan Y, Tavakkoli E, Wang X, Zhang R. 2021. Priming, stabilization and temperature sensitivity of native SOC is controlled by microbial responses and physicochemical

properties of biochar. *Soil Biology and Biochemistry*, **154**, 108139.
Cheng W, Parton W J, Gonzalez-Meler M A, Phillips R, Asao S, McNickle G, Brzostek E, Jastrow J. 2014. Synthesis and modeling perspectives of rhizosphere priming. *New Phytologist*, **201**, 31–44.
Creamer C A, de Menezes A B, Krull E S, Sanderman J, New-ton-Walters R, Farrell M. 2015. Microbial community structure mediates response of soil C decomposition to litter addition and warming. *Soil Biology and Biochemistry*, **80**, 175–188.
Crowther T W, Todd-Brown K E O, Rowe C W, Wieder W R, Carey J C, Machmuller M B, Snoek B L, Fang S, Zhou G, Allison S D, Blair J M, Bridgham S D, Burton A J, Carrillo Y, Reich P B, Clark J S, Classen A T, Dijkstra F A, Elberling B, Emmett B A, *et al.* 2016. Quantifying global soil carbon losses in response to warming. *Nature*, **540**, 104–108.
Cui J, Wei L, Zhu Z K, Deng Y W, Chen S, Kuzyakov Y, Ge T D. 2024. Influence of soil N availability on priming effects depending on temperature. *Soil Tillage Research*, **242**, 106163.
Cui J, Zhu Z, Xu X, Liu S, Jones D L, Kuzyakov Y, Shibistova O, Wu J, Ge T. 2020. Carbon and nitrogen recycling from microbial necromass to cope with C:N stoichiometric imbalance by priming. *Soil Biology and Biochemistry*, **142**, 107720.
Cui Y, Fang L, Guo X, Wang X, Zhang Y, Li P, Zhang X. 2018. Ecoenzymatic stoichiometry and microbial nutrient limitation in rhizosphere soil in the arid area of the northern Loess Plateau, China. *Soil Biology and Biochemistry*, **116**, 11–21.
Davis K E R, Sangwan P, Janssen P H. 2011. *Acidobacteria*, *Rubrobacteridae* and *Chloroflexi* are abundant among very slow growing and mini-colony-forming soil bacteria. *Environmental Microbiology*, **13**, 798–805.
Ding J X, He Y H, Yin L M, Huang C J, Xue K, Yan S B, Liu R Q, Wang P, Zhou X H. 2025. Divergent responses of soil positive and negative priming effects to experimental warming. *Global Ecology and Biogeography*, **34**, e70028.
Dong H, Lin J, Lu J, Li L, Yu Z, Kumar A, Zhang Q, Liu D, Chen B. 2022. Priming effects of surface soil organic carbon decreased with warming: A global meta-analysis. *Plant and Soil*, **500**, 233–242.
Dong M Q, Zhao J, Li E, Liu Z J, Guo S B, Zhang Z T, Cui W Q, Yang X G. 2023. Effects of changing climate extremes on maize grain yield in Northeast China. *Agronomy*, **13**, 1050.
Douglas G M, Mafei V J, Zaneveld J, Yurgel S N, Brown J R, Taylor C M, Huttenhower C, Langille M G I. 2019. PICRUSt2: An improved and extensible approach for metagenome inference. *BioRxiv*, doi: https://doi.org/10.1101/672295.
Eilers K G, Lauber C L, Knight R, Fierer N. 2010. Shifts in bacterial community structure associated with inputs of low molecular weight carbon compounds to soil. *Soil Biology and Biochemistry*, **42**, 896–903.
Fang Y, van Zwieten L, Rose M T, Vasileiadis S, Donner E, Vancov T, Rigg J L, Weng Z, Lombi E, Drigo B, Conyers M, Tavakkoli E. 2022. Unraveling microbiomes and functions associated with strategic tillage, stubble, and fertilizer management. *Agriculture*, *Ecosystems & Environment*, **323**, 107686.
Fanin N, Alavoine G, Bertrand I. 2020. Temporal dynamics of litter quality, soil properties and microbial strategies as main drivers of the priming effect. *Geoderma*, **377**, 114576.
Feng J G, Tang M, Zhu B. 2021. Soil priming effect and its responses to nutrient addition along a tropical forest elevation gradient. *Global Change Biology*, **27**, 2793–2806.
Fierer N, Bradford M A, Jackson A R B. 2007. Toward an ecological classification of soil bacteria. *Ecology*, **88**, 1354–1364.
Fontaine S, Bardoux G, Abbadie L, Mariotti A. 2004. Carbon input to soil may decrease soil carbon content. *Ecology Letters*, **7**, 314–320.
Fu Y Y, Liu W L, Chen Z Y, Redmile-Gordon M, Liang C, Tang C, Guggenberger G, Yan S B, Yin L M, Peng J J, Zwieten L V, Wang P, Chen J, Kuzyakov Y, Ge T D, Xu J M, Luo Y. 2025. Microbial metabolisms determine soil priming effect induced by organic inputs. *Soil Biology and Biochemistry*, **209**, 109885.
Ghee C, Neilson R, Hallett P D, Robinson D, Paterson E. 2013. Priming of soil organic matter mineralization is intrinsically insensitive to temperature. *Soil Biology and Biochemistry*, **66**, 20–28.
Guo L, Yu Z, Li Y, Xie Z, Wang G, Liu J, Hu X, Wu J, Liu X, Jin J. 2023. Stimulation of primed carbon under climate change corresponds with phosphorus mineralization in the rhizosphere of soybean. *Science of the Total Environment*, **899**, 165580.
Guttières R, Nunan N, Raynaud X, Lacroix G, Barot S, Barré P, Girardin C, Guenet B, Lata J C, Abbadie L. 2021. Temperature and soil management effects on carbon fluxes and priming effect intensity. *Soil Biology and Biochemistry*, **153**, 108103.
Hou Z N, Liu W Z, Xu S Q, Chang S, Zhang X J, Wang R H, Luo D Q, Wang B R, An S S, Qiao Y H, Du Z L, Wei Y Q. 2025. Warming-induced response of microbial diversity and functions regulated microbial necromass and soil multifunctionality. *Applied Soil Ecology*, **206**, 105798.
Huang Q, Wang B R, Shen J K, Xu F J, Li N, Jia P H, Jia Y J, An S S, Amoah I D, Huang Y M. 2024. Shifts in C-degradation genes and microbial metabolic activity with vegetation types affected the surface soil organic carbon pool. *Soil Biology and Biochemistry*, **192**, 109371.
Huo C F, Luo Y Q, Cheng W X. 2017. Rhizosphere priming effect: a meta-analysis. *Soil Biology and Biochemistry*, **111**, 78–84.
Jenkinson D S, Brookes P C, Powlson D S. 2004. Measuring soil microbial biomass. *Soil Biology and Biochemistry*, **36**, 5–7.
Kaiser C, Franklin O, Dieckmann U, Richter A. 2014. Microbial community dynamics alleviate stoichiometric constraints during litter decay. *Ecology Letters*, **7**, 680–690.
Karimi B, Maron P A, Chemidlin-Prevost Boure N, Bernard N, Gilbert D, Ranjard L. 2017. Microbial diversity and ecological networks as indicators of environmental quality. *Environmental Chemistry Letters*, **15**, 265–281.
Khodadad C L M M, Zimmerman A R, Green S J, Uthandi S, Foster J S. 2011. Taxa-specific changes in soil microbial community composition induced by pyrogenic carbon amendments. *Soil Biology and Biochemistry*, **43**, 385–392.
Kuzyakov Y. 2010. Priming effects: Interactions between living and dead organic matter. *Soil Biology and Biochemistry*, **42**, 1363–1371.
Kuzyakov Y, Mason-Jones K. 2018. Viruses in soil: Nano-scale undead drivers of microbial life, biogeochemical turnover and ecosystem functions. *Soil Biology and Biochemistry*, **127**, 305–317.
Lehmann J, Kleber M. 2015. The contentious nature of soil organic matter. *Nature*, **528**, 60–68.
Li G L, Chen X F, Qin W J, Chen J R, Leng K, Sun L Y, Liu M, Wu M, Fan J B, Xu C X, Liu J. 2024. Characteristics of the microbial communities regulate soil multi-functionality under different cover crop amendments in Ultisol. *Journal of Integrative Agriculture*, **23**, 2099–2111.
Li H, Yang S, Semenov M V, Yao F, Ye J, Bu R, Ma R, Lin J, Kurganova I, Wang X, Deng Y, Kravchenko I, Jiang Y, Kuzyakov Y. 2021. Temperature sensitivity of SOM decomposition is linked with a K-selected microbial community. *Global Change Biology*, **27**, 2763–2779.
Li L, Zhu-Barker X, Ye R, Doane T A, Horwath W R. 2018. Soil microbial biomass size and soil carbon influence the priming effect from carbon inputs depending on nitrogen availability. *Soil Biology and Biochemistry*, **119**, 41–49.
Li X, Feng J, Zhang Q, Zhu B. 2023. Warming inhibits the priming effect of soil organic carbon mineralization: A meta-analysis. *Science of the Total Environment*, **904**, 166170.
Liang C, Amelung W, Lehmann J, Kastner M. 2019. Quantitative assessment of microbial necromass contribution to soil organic matter. *Global Change Biology*, **25**, 3578–3590.
Liang Y, Cao D, Ma Z, Wu R, Zhang H, Fang Y, Shahbaz M, Liu X J A, Kuzyakov Y, Chen J, Ge T. 2024. Stoichiometry regulates rice straw-induced priming effect: The microbial life strategies. *Soil Biology and Biochemistry*, **196**, 109514.
Lyu L H, Wang C Q, Fan K K, Li J S, Yang T, Gao G F, Sun R, Wang J, Xu X Y, Zhang Y X, Ma Y Y, Zhang J B, Kuzyakov Y, Chu H Y. 2025. Microbial life-history strategies mediate temperature effects on organic carbon pools in black soils. *Soil Ecology Letters*, **7**, 250306.
Ma S, Zhu W, Wang W, Li X, Sheng Z. 2023. Microbial assemblies with distinct trophic strategies drive changes in soil microbial carbon use efficiency along vegetation primary succession in a glacier retreat area of the southeastern Tibetan Plateau. *Science of the Total Environment*, **867**, 161587.
Paul E A. 2007. *Soil Microbiology*, *Ecology*, *and Biochemistry*. Academic Press, New York.
Pausch J, Holz M, Zhu B, Cheng W X. 2024. Rhizosphere priming promotes plant nitrogen acquisition by microbial necromass recycling. *Plant*, *Cell & Environment*, **47**, 1987–1996.

Pingthaisong W, Blagodatsky S, Vityakon P, Cadisch G. 2024. Mixing plant residues of different quality reduces priming effect and contributes to soil carbon retention. *Soil Biology and Biochemistry*, **188**, 109242.

Razanamalala K, Razafimbelo T, Maron P A, Ranjard L, Chemidlin N, Lelievre M, Dequiedt S, Ramaroson V H, Marsden C, Becquer T, Trap J, Blanchart E, Bernard L. 2018. Soil microbial diversity drives the priming effect along climate gradients: A case study in Madagascar. *ISME Journal*, **12**, 451–462.

Reji L, Darnajoux R, Zhang X N. 2024. A genomic view of environmental and life history controls on microbial nitrogen acquisition strategies. *Environmental Microbiology Reports*, **16**, e13220.

Ren C, Wang J, Bastida F, Delgado-Baquerizo M, Yang Y, Wang J, Zhong Z, Zhou Z, Zhang S, Guo Y, Zhou S, Wei G, Han X, Yang G, Zhao F. 2022. Microbial traits determine soil C emission in response to fresh carbon inputs in forests across biomes. *Global Change Biology*, **28**, 1516–1528.

Ren T, Huang X, Sun H, Xie H, Jia Z, Wang J. 2025. Comparison on responses of black soil microorganisms to exogenous carbon and nitrogen addition under no-tillage with straw mulching and combined application of organic and inorganic fertilizers. *Acta Microbiologica Sinica*, **65**, 3348–3364. (in Chinese)

Song X, Liu X, Liang G, Li S, Li J, Zhang M, Zheng F, Ding W, Wu X, Wu H. 2022. Positive priming effect explained by microbial nitrogen mining and stoichiometric decomposition at different stages. *Soil Biology and Biochemistry*, **175**, 108852.

Tan F, Cheng J, Zhang Y, Jiang X, Liu Y. 2022. Genomics analysis and degradation characteristics of lignin by *Streptomyces thermocarboxydus* strain DF3-3. *Biotechnology for Biofuels and Bioproducts*, **15**, 1–15.

Tao X Y, Yang Z F, Feng J J, Jian S Y,Yang Y F, Bates C T, Wang G S, Guo X, Ning D L, Kempher M L, Liu X J A, Ouyang Y, Han S, Wu L W, Zeng Y F, Kuang J L, Zhang Y, Zhou X S, Shi Z, Qin W, *et al.* 2024. Experimental warming accelerates positive soil priming in a temperate grassland ecosystem. *Nature Communications*, **15**, 1178.

Tian Q, Jiang Q, Zhao R, Wu Y, Lin Q, Zhao X, Tang Z, Liu F. 2023. Microbial properties control soil priming and exogenous carbon incorporation along an elevation gradient. *Geoderma*, **431**, 116343.

Tong Y X, Liu J G, Li X L, Sun J, Herzberger A, Wei D, Zhang W F, Dou Z X, Zhang F S. 2017. Cropping system conversion led to organic carbon change in China's Mollisols regions. *Scientific Report*, **7**, 18064.

Vance E D, Brookes P C, Jenkinson D S. 1987. An extraction method for measuring soil microbial biomass C. *Soil Biology and Biochemistry*, **19**, 703–707.

Wagg C, Schlaeppi K, Banerjee S, Kuramae E E, van der Heijden M G A. 2019. Fungalbacterial diversity and microbiome complexity predict ecosystem functioning. *Nature Communications*, **10**, 4841.

Wang J, Pan F, Soininen J, Heino J, Shen J. 2016. Nutrient enrichment modifies temperature biodiversity relationships in large-scale field experiments. *Nature Communications*, **7**, 13960.

Wang J, Yao H Y, Zhang X. 2024. The effect of the ^{13}C abundance of soil microbial DNA on identifying labelled fractions after ultracentrifugation. *Applied Microbiology and Biotechnology*, **108**, 318.

Xu Q, Jin J, Wang X, Armstrong R, Tang C. 2019. Susceptibility of soil organic carbon to priming after long-term CO_2 fumigation is mediated by soil texture. *Science of the Total Environment*, **657**, 1112–1120.

Yanni S F, Diochon A, Helgason B L, Ellert B H, Gregorich E G. 2018. Temperature response of plant residue and soil organic matter decomposition in soil from different depths. *European Journal of Soil Science*, **69**, 325–335.

You M, He P, Dai S, Burger M, Li L J. 2021. Priming effect of stable C pool in soil and its temperature sensitivity. *Geoderma*, **401**, 115216.

Yu X Y, Ma Y Y. 2022. Spatial and temporal analysis of extreme climate events over Northeast China. *Atmosphere*, **13**, 1197.

Yu Z Y, Ling L, Singh BP, Luo Y, Xu J M. 2020. Gain in carbon: Deciphering the abiotic and biotic mechanisms of biochar-induced negative priming effects in contrasting soils. *Science of the Total Environment*, **746**, 141057.

Zhang H, Chang D, Zhu Z, Meng C, Wang K. 2024. Soil priming effects and involved microbial community along salt gradients. *Biogeosciences*, **21**, 1–11.

Zhang T T, Liu Y L, Ge S Q, Peng P, Tang H, Wang J W. 2024. Sugarcane/soybean intercropping with reduced nitrogen addition enhances residue-derived labile soil organic carbon and microbial network complexity in the soil during straw decomposition. *Journal of Integrative Agriculture*, **23**, 4216–4236.

Zhao F, Wang J, Li Y, Xu X, He L, Wang J, Ren C, Guo Y. 2022. Microbial functional genes driving the positive priming effect in forest soils along an elevation gradient. *Soil Biology and Biochemistry*, **165**, 108498.

Zhao J, Xie X, Jiang Y, Li J, Fu Q, Qiu Y, Fu X, Yao Z, Dai Z, Qiu Y. 2024. Effects of simulated warming on soil microbial community diversity and composition across diverse ecosystems. *Science of the Total Environment*, **911**, 168793.

Zheng Y, Wang X, Hayden H, Franks A, Shindler A, Liu Y, Clark G, Jin J, Tang C. 2023. Soil types differ in the temporal response of the priming effect to N addition: A study on microbial mechanisms. *Biology and Fertility of Soils*, **59**, 233–247.

Zhong Z K, Li W J, Lu X Q, Gu Y Q, Wu S J, Shen Z Y, Han X H, Yang G H, Ren C J. 2020. Adaptive pathways of soil microorganisms to stoichiometric imbalances regulate microbial respiration following afforestation in the Loess Plateau, China. *Soil Biology and Biochemistry*, **151**, 108048.

Zhou J, Liu Y, Liu C Y, Zamanian K, Feng W H, Steiner S K, Shi L L, Guillaume T, Kumar A. 2024. Necromass responses to warming: A faster microbial turnover in favor of soil carbon stabilisation. *Science of the Total Environment*, **954**,176651.

Zhou S, Wang J, Chen L, Wang J, Zhao F. 2022. Microbial community structure and functional genes drive soil priming effect following afforestation. *Science of the Total Environment*, **825**, 153925.

Zhu Z, Fang Y, Liang Y, Li Y, Liu S, Li Y, Li B, Gao W, Yuan H, Kuzyakov Y, Wu J, Richter A, Ge T. 2022. Stoichiometric regulation of priming effects and soil carbon balance by microbial life strategies. *Soil Biology and Biochemistry*, **169**, 108669.

Executive Editor-in-Chief Keke Yi
Managing Editor Lujuan Sun